

# Misfolded G $\beta$ is recruited to cytoplasmic dynein by Nudel for efficient clearance

Yihan Wan<sup>1</sup>, Zhenye Yang<sup>1</sup>, Jing Guo<sup>1</sup>, Qiangge Zhang<sup>1</sup>, Liyong Zeng<sup>1</sup>, Wei Song<sup>1</sup>, Yue Xiao<sup>1</sup>, Xueliang Zhu<sup>1</sup>

<sup>1</sup>State Key Laboratory of Cell Biology, Institute of Biochemistry and Cell Biology, Shanghai Institutes for Biological Sciences, Chinese Academy of Sciences, 320 Yue Yang Road, Shanghai 200031, China

The G $\beta\gamma$  heterodimer is an important signal transducer. G $\beta$ , however, is prone to misfolding due to its requirement for G $\gamma$  and chaperones for proper folding. How cells dispose of misfolded G $\beta$  (mfG $\beta$ ) is not clear. Here, we showed that mfG $\beta$  was able to be polyubiquitinated and subsequently degraded by the proteasome. It was sequestered in aggresomes after the inhibition of the proteasome activity with MG132. Sustained activation of G $\beta\gamma$  signaling further elevated cellular levels of the ubiquitinated G $\beta$ . Moreover, Nudel, a regulator of cytoplasmic dynein, the microtubule minus end-directed motor, directly interacted with both the unubiquitinated and ubiquitinated mfG $\beta$ . Increasing the levels of both mfG $\beta$  and Nudel promoted the association of G $\beta$  with both Nudel and dynein, resulting in robust aggresome formation in a dynein-dependent manner. Depletion of Nudel by RNAi reduced the dynein-associated mfG $\beta$ , impaired the MG132-induced aggresome formation, and markedly prolonged the half-life of nascent G $\beta$ . Therefore, cytosolic mfG $\beta$  is recruited to dynein by Nudel and transported to the centrosome for rapid sequestration and degradation. Such a process not only eliminates mfG $\beta$  efficiently for the control of protein quality, but may also help to terminate the G $\beta\gamma$  signaling.

**Keywords:** protein degradation; dynein-mediated transport; G $\beta$ ; protein misfolding; signaling

*Cell Research* (2012) 22:1140-1154. doi:10.1038/cr.2012.41; published online 20 March 2012

## Introduction

The heterotrimeric G proteins are signal transducers of the G protein-coupled receptors (GPCRs). The activation of GPCR by an agonist leads to the dissociation of G $\beta\gamma$ , a tightly bound dimer formed by the G $\beta$  and G $\gamma$  subunits, from G $\alpha$  and the subsequent activation of downstream effectors [1-4]. The G proteins also function as transducers of polarity information in a GPCR-independent manner. For instance, during asymmetric cell division, the activator of the G-protein signaling (AGS) family proteins, including LGN (also named AGS5), can bind directly to G $\alpha$ , leading to the dissociation of G $\beta\gamma$  from G $\alpha$  [5-7]. After the G protein signaling is terminated, free G $\alpha$  may be recycled back to the plasma membrane [8]. However, the fate of free G $\beta\gamma$  is not clear. The long-term activation

of  $\mu$ -opioid receptor, a GPCR, has been shown to induce the proteasome-dependent degradation of G $\beta$  [9]. Furthermore, the turnover rate of G $\beta$  is positively correlated with G $\beta\gamma$  levels [10]. Therefore, there may be a feedback degradation mechanism to avoid excessive G $\beta\gamma$  signaling.

G $\beta$  is prone to misfolding. Its proper conformation and subcellular localization depend on G $\gamma$  [2, 3, 8]. Only 30%-50% of *in vitro* translated G $\beta$  and G $\gamma$  form functional G $\beta\gamma$  dimers [4]. In fact, efficient formation of G $\beta\gamma$  from newly synthesized G $\beta$  and G $\gamma$  also requires the CCT chaperone complex and the phosphatidylethanolamine transferase-like protein (PhLP1) [4, 8]. A stoichiometric excess of G $\beta$  over G $\gamma$ , as in the case of G $\beta$  overexpression, should also lead to misfolding. However, the mechanism of how the cells dispose of misfolded G $\beta$  (mfG $\beta$ ) remains elusive.

The proteasome is a large, multi-subunit protein complex that can degrade unwanted proteins into small peptides. Before degradation, the substrates for the proteasome are subjected to polyubiquitination. It is estimated that ~20% of nascent polypeptides are degraded, presumably due to a failure to satisfy the cellular quality control machinery [11]. As misfolding often results in

Correspondence: Xueliang Zhu

Tel: 86-21-54921406; Fax: 86-21-54921011

E-mail: xlzhu@sibs.ac.cn

Received 30 October 2011; revised 29 January 2012; accepted 12 February 2012; published online 20 March 2012

the exposure of hydrophobic regions that are normally buried inside the protein, misfolded proteins tend to aggregate. Excess protein aggregates are sometimes transported by cytoplasmic dynein, a microtubule (MT)-based motor, to the MT-organizing center (MTOC), where the centrosome resides. There, they form a large juxtannuclear inclusion, termed an aggresome. Aggresome formation sequesters protein aggregates from the cytosol to possibly reduce their potential cytotoxic effects. Aggresomes can also trigger autophagy, an intracellular “engulfing” process that degrades membrane organelles and large protein inclusions. Components of the ubiquitin (Ub)-proteasome system (UPS) and several chaperones are usually enriched in aggresomes to facilitate the elimination of misfolded proteins by degradation or refolding [11-14].

The mechanism by which different protein aggregates are loaded onto the dynein motor is still poorly understood. Cytoplasmic dynein is a very large protein complex containing two heavy chains (DHC), several intermediate (DIC), light intermediate, and light chains. Its association with many membrane cargos or target sites requires another protein complex, dynactin [15, 16]. Huntingtin-associated protein may mediate the association between huntingtin aggregates and the dynein motor by binding to the p150<sup>Glued</sup> subunit of dynactin [17]. Histone deacetylase 6 (HDAC6) has been proposed to regulate aggresome formation by linking ubiquitinated proteins to dynein [18], though whether HDAC6 directly interacts with dynein or dynactin is not clear.

Nudel (also called Ndel1) is a dynein-interacting protein that is critical for a variety of dynein functions *in vivo* [19-24]. In this report, we show that in addition to its regulatory function, Nudel also serves as an adaptor for mfG $\beta$  on dynein to facilitate the sequestration of mfG $\beta$ . We also provide evidence for the negative regulation of G $\beta\gamma$  signaling via the degradation of G $\beta$  through the ubiquitin proteasome pathway.

## Results

### *Nudel interacts directly with G $\gamma$ -free G $\beta$*

To further understand Nudel function, a yeast two-hybrid screen was performed to identify novel Nudel-associated proteins. The bait plasmid, pAS2-Nudel, was constructed to express full-length Nudel fused with the DNA-binding domain of Gal4. This plasmid was transformed with a pACT2-based human placenta cDNA library (Clontech) into the yeast strain Y190. The plasmid isolated from a positive clone contained a full-length cDNA for G $\beta$ 2, one of the five G $\beta$  subtypes in mammals [3]. The result of the screen was further confirmed by the

co-transfection of pACT2-G $\beta$ 2 with either pAS2-Nudel or the vector (pAS2-1) alone (Figure 1A). Direct interaction of His-tagged G $\beta$ 2 with Flag-tagged Nudel, but not with the control protein, E2F1, was then confirmed by *in vitro* binding assays using bacterially expressed proteins (Figure 1B). The latter result also suggests that G $\gamma$  is not required for the Nudel-G $\beta$ 2 interaction.

We then performed co-immunoprecipitation (co-IP) analysis with HEK293T cells. As the anti-G $\gamma$  antibodies in our hands were not sensitive enough to detect the low-level expressions of endogenous G $\gamma$  in the HEK293T cell lysate (Supplementary information, Figure S1), we overexpressed G $\gamma$ 2, which has a strong affinity to G $\beta$ 2 and is also able to heterodimerize with all of the other G $\beta$  subtypes, except G $\beta$ 3 [25, 26], to facilitate its detection by the anti-G $\gamma$ 2 antibody. When Flag-Nudel was co-expressed (Figure 1C, lane 1), co-IP using the anti-Flag M2 resin indicated an association of endogenous G $\beta$  with Flag-Nudel (Figure 1C, lane 3). As expected, G $\gamma$ 2, Gai and Gas were not detected in the immunocomplex (Figure 1C, lane 3). We further demonstrated the association between endogenous Nudel and G $\beta$  *in vivo* by co-IP with either anti-Nudel IgY or anti-G $\beta$  IgG (Figure 1D, lanes 3 and 5). Together, these results revealed that Nudel directly interacts *in vivo* with G $\gamma$ -free G $\beta$ , which is presumably unfolded or misfolded [2, 3].

To map interaction regions, a series of Nudel or G $\beta$ 2 mutants were constructed (Figure 1E-1F). Co-IP showed that the N-terminal 201 residues of Nudel (Nudel<sup>P2N</sup>) associated with G $\beta$ 2, whereas further depletion of the first 55 (Nudel<sup>P2N2</sup>) or the last 35 residues (Nudel<sup>P2N3</sup>) abolished the interaction (Figure 1E and Supplementary information, Figure S2A). Nudel<sup>P2N</sup> contains the “QXXER” motif at residues 145-149, which is highly conserved in Nudel family proteins from fungi, such as *Aspergillus*, to vertebrates (Supplementary information, Figure S2A). This motif was originally identified in several G $\beta\gamma$  effectors and is important for the association of adenylyl cyclase 2 (AC2) with G $\beta$  [27, 28]. When the motif in Nudel<sup>P2N</sup> was mutated (QAIER→AAILV), the resultant protein, Nudel<sup>P2Nm</sup>, showed a weaker association with His-G $\beta$ 2 (Figure 1E and Supplementary information, Figure S2A). Conversely, Nudel associated with G $\beta$ 2M and G $\beta$ 2C, which contained the 2nd-4th and 5th-7th WD repeats, respectively, but not with G $\beta$ 2N, which contained residues 1-68 (Figure 1F and Supplementary information, Figure S2B). As all G $\beta$  subtypes in mammals share similar structural characteristics [2, 3], we further overexpressed HA-tagged G $\beta$ 1,  $\beta$ 4, or  $\beta$ 5 and found that, like HA-G $\beta$ 2, they also associated with Flag-Nudel in the co-IP assays (Figure 1G).

Taken together, we conclude that Nudel directly in-

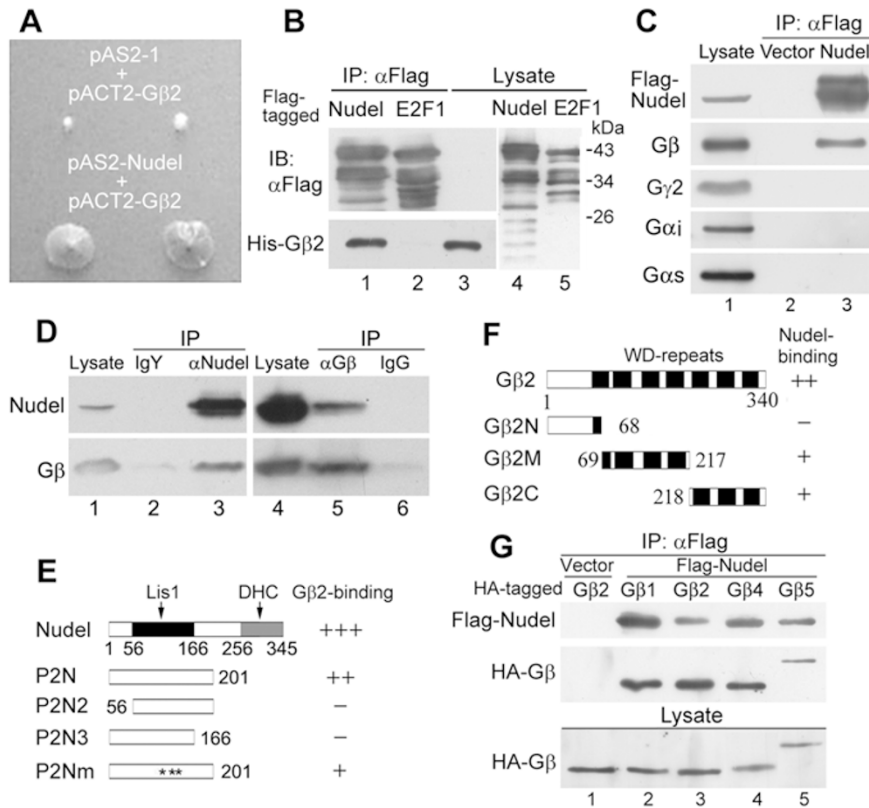


**Figure 1** Interaction of G $\gamma$ -free G $\beta$  with Nudel. **(A)** The interaction assessed in a yeast two-hybrid system. pAS2-1 and pACT2 are vectors harboring the DNA-binding domain and activation domain of Gal4, respectively. Yeast cells transformed with the indicated plasmids were initially selected on synthetic dropout medium lacking leucine and tryptophan at 30 °C. Colonies were subsequently inoculated on medium further lacking histidine. The growth of colonies suggests protein interaction. **(B)** *In vitro* binding assays using the bacterially expressed proteins. Flag-E2F1 was used as a negative control. IP, immunoprecipitation; IB, immunoblotting. **(C)** The interaction of Flag-Nudel with G $\gamma$ 2-free G $\beta$  *in vivo*. HEK293T cells transfected to overexpress Flag-Nudel and G $\gamma$ 2 (lane 1) or G $\gamma$ 2 alone were lysed in co-IP buffer (see Materials and Methods) and subjected to co-IP (lanes 2-3) using anti-Flag M2 resin. IB was then performed to visualize the indicated proteins. **(D)** The *in vivo* interaction between endogenous Nudel and G $\beta$ . The HEK293T cell lysates (lanes 1, 4) were subjected to co-IP using a control IgY (lane 2), anti-Nudel IgY (lane 3), anti-G $\beta$  antibody (lane 5), or normal IgG (lane 6). **(E, F)** The mapping of the binding domains. The diagrams of Nudel, G $\beta$ 2, and the mutants, together with their binding abilities as assessed by co-IP, are shown. Also see Supplementary information, Figure S2 for the corresponding IB results. The asterisks in P2Nm indicate that the QAIER motif was mutated to AAILV. **(G)** The association of Flag-Nudel with HA-tagged G $\beta$  subtypes. Co-IP was performed with the lysates of HEK293T cells overexpressing the indicated proteins. G $\beta$ 3 was not examined due to the lack of its cDNA.

teracts with the WD repeats of G $\beta$  that is free of  $\alpha$  and  $\gamma$  subunits. As Nudel differs from other G $\beta$  interactors that bind to the G $\beta$  $\gamma$  heterodimer [1, 4], we speculate that it may regulate the clearance of mfG $\beta$  rather than physiological functions of G $\beta$  $\gamma$ .

*Nudel promotes the accumulation of mfGβ at the centrosome region*

To gain insights into the biological significance of the Nudel-G $\beta$  interaction, we examined their potential interplays in COS-7 cells. As shown in previous studies [29-31], GFP-Nudel localized at the centrosome (Figure

2A, panel 1). His-G $\beta$ 2 exhibited centrosome localization in 43.2%  $\pm$  1.6% of transfected cells ( $n = 317$ , two experiments) (Figure 2A, panel 2, arrow), though it also formed aggregates of varying sizes and numbers (Figure 2A, panel 2). In addition to His-G $\beta$ 2, RFP-G $\beta$ 2 also showed the similar centrosomal localization (Supplementary information, Figure S3A). Moreover, although endogenous G $\beta$  is typically plasma membrane-localized [5-7], permeabilization briefly with Triton X-100 (0.1%) prior to the fixation facilitated the detection of its centrosome localization in COS-7 and HeLa cells (Supplementary information, Figure S3B), indicating that such

a centrosomal localization is an intrinsic property of G $\beta$ . Surprisingly, overexpression of both GFP-Nudel and His-G $\beta$ 2 (Figure 2B) led to the formation of a large aggregate containing both proteins at the centrosome region (Figure 2A, panels 3-4) in approximately 60% of cells ( $n = 356$ ), reminiscent of aggresomes in morphology [32]. As Nudel interacted with all the G $\beta$  isoforms that we examined (Figure 1G), we coexpressed GFP-Nudel with HA-tagged G $\beta$ 1, G $\beta$ 2, G $\beta$ 4, or G $\beta$ 5 and observed the similar aggregate formation at the centrosomal region (Supplementary information, Figure S4).

We then investigated whether the large centrosomal aggregates were the aggresomes. The aggresome is surrounded by cage-like vimentin structures, due to the rear-

angement of vimentin-containing intermediate filaments [12, 32], and is often rich in ubiquitin, due to the polyubiquitination of misfolded proteins [18, 32]. We coexpressed GFP-Nudel and RFP-G $\beta$ 2 to facilitate multi-color fluorescence microscopy and found that they formed centrosomal aggregates, which were indeed surrounded by the cage-like vimentin structures (Figure 2C, panels 1-2, arrows). Moreover, the aggregates were labeled by anti-Ub antibody (Figure 2C, panels 3-4, arrows), suggesting the enrichment of ubiquitinated protein(s). When G $\gamma$ 2 was coexpressed, it predominantly displayed membrane localization and was absent in the aggregates (Figure 2C, panels 5-6), indicating that the G $\beta$ 2 in the aggregates is free of G $\gamma$  and thus misfolded. Together, these

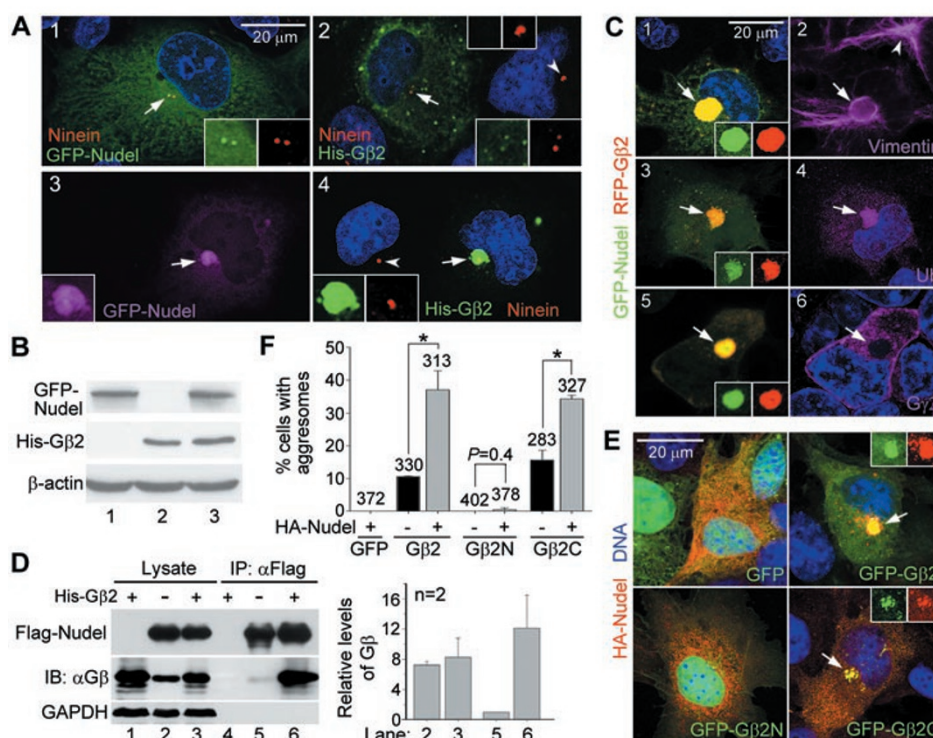


**Figure 2** G $\beta$ 2 forms aggresomes when overexpressed with Nudel. **(A)** GFP-Nudel and His-G $\beta$ 2 were overexpressed either separately (panels 1-2) or together (panels 3-4) in COS-7 cells. The centrosomes marked by ninein staining are indicated by the arrows in the transfected cells or arrowheads in the untransfected cells. Typical centrosome regions are magnified 2 $\times$  to show details. Nuclear DNA is shown in blue. **(B)** The relative expression levels of GFP-Nudel and His-G $\beta$ 2 in COS-7 cells. **(C)** The centrosomal aggregates formed by exogenous Nudel and G $\beta$ 2 (arrows) were aggresomes. COS-7 cells were transfected to express GFP-Nudel and RFP-G $\beta$ 2. The cells were immunostained to visualize vimentin (panels 1-2) or Ub (panels 3-4). In panels 5-6, G $\gamma$ 2 was further overexpressed to facilitate its detection by the anti-G $\gamma$ 2 antibody, which did not have enough affinity to detect endogenous G $\gamma$ 2 in cultured cells (see Supplementary information, Figure S1). The arrows point to the positions of the aggresomes. The arrowhead in panel 2 denotes vimentin staining in an untransfected cell. The insets show the fluorescence of individual proteins. Nuclear DNA is shown in blue. **(D)** Overexpression of G $\beta$ 2 dramatically stimulated the Nudel-G $\beta$  interaction. Flag-Nudel was overexpressed alone or with His-G $\beta$ 2 in HEK293T cells. 1/40 of input or 1/10 of the co-IP eluate was loaded in each lane. **(E, F)** The aggresome formation of exogenous G $\beta$ 2 required the Nudel-G $\beta$  interaction. HA-Nudel was coexpressed with the indicated GFP fusion proteins in COS-7 cells. The arrows indicate the aggresomes. The statistical results were from two independent experiments. The total numbers of counted cells are listed above the histograms. \*indicates  $P < 0.05$  in Student's  $t$ -test.



results indicate that Nudel and mfG $\beta$  form aggresomes upon their co-overexpression.

To understand whether the aggresome formation was correlated with increased Nudel-G $\beta$  interaction, we used Flag-Nudel to immunoprecipitate G $\beta$  from HEK293T cells. We found that, although overexpression of His-G $\beta$ 2 did not significantly increase the total levels of G $\beta$  (Figure 2D, lane 3 vs 2), the amount of G $\beta$  associated with Flag-Nudel increased by an average of 12.1-fold (lane 6 vs 5). Such a result is consistent with the stoichiometric requirement of both Nudel and G $\beta$ 2 for the aggresome formation (Figure 2A-2C) and also suggests that the overexpression of His-G $\beta$ 2 markedly increases the total levels of mfG $\beta$ . Provided that all the mfG $\beta$  was precipitated in the co-IP experiments, the overexpression of His-G $\beta$ 2 was estimated to increase the levels of mfG $\beta$  by approximately 10-fold, from  $0.3\% \pm 0.1\%$  to  $3.1\% \pm 0.3\%$  of the total G $\beta$ .

To further confirm the specificity of the aggresome formation, we coexpressed HA-Nudel with GFP or GFP-tagged G $\beta$ 2 or its mutants (Figure 2E). Statistical analyses indicated that GFP-G $\beta$ 2 or GFP-G $\beta$ 2C, a deletion mutant capable of binding to Nudel (Figure 1F and Supplementary information, Figure S2B), alone formed the aggresome-like aggregates in an average of 10.6% or 15.7% of cells, the coexpression of HA-Nudel increased the incidence of the aggresome formation to 37.1% and 34.4%, respectively (Figure 2E and 2F). However, neither GFP nor GFP-G $\beta$ 2N, a truncation mutant showing no interaction with Nudel (Figure 1F and Supplementary information, Figure S2B), exhibited the aggresome formation, regardless of the expression of HA-Nudel (Figure 2E and 2F). Taken together, we conclude that Nudel facilitates the centrosome accumulation of mfG $\beta$  in their interaction-dependent manner.

#### *The aggresome formation of G $\beta$ 2 requires cytoplasmic dynein activity*

To understand how the G $\beta$ 2 aggresome was formed, we examined the dynamics of RFP-G $\beta$ 2 in the presence of GFP-Nudel or GFP in live cells. To monitor early events, COS-7 cells that were transfected for 12 h, at which time the accumulation of RFP-G $\beta$ 2 at the juxtannuclear region was still not significant (Figure 3A), were imaged at 3-min intervals for at least 240 min. In the control cells overexpressing GFP, RFP-G $\beta$ 2 failed to show an enrichment at the juxtannuclear region over time, whereas in the presence of GFP-Nudel, small RFP-G $\beta$ 2 aggregates gradually accumulated at the centrosome (Figure 3A, arrows; Figure 3B).

As Nudel is a dynein regulator, we examined whether dynein contributed to the G $\beta$ 2 aggresome formation. We

found that both dynein (DIC) and dynactin (p150<sup>Glued</sup>) were enriched at the aggresomes (Figure 3C, arrows). Moreover, when GFP-Nudel and His-G $\beta$ 2 were co-overexpressed with Flag-tagged p50, a dynactin subunit that inactivates dynein upon its overexpression [33], the aggresome formation was abolished in 91% ( $n = 448$ , two experiments) of the triple positive cells. In these cells, exogenous Nudel and G $\beta$ 2 only exhibited basal-level centrosome localizations (Figure 3D, arrow). Immunoblotting (IB) indicated that p50 overexpression had no effect on the protein levels of Nudel and G $\beta$  (Supplementary information, Figure S5). Therefore, the loss of G $\beta$  aggresome formation (Figure 3D) was attributed to the inactivation of dynein instead of decreased Nudel or G $\beta$  levels. The His-G $\beta$ 2 remaining at the centrosome (Figure 3D) may be due to residual dynein activity or to the direct association of G $\beta$ 2 with centrosomal Nudel, which is dynein-independent [31].

To corroborate the above results, we used erythro-9-(3-(2-hydroxyethyl)adenine (EHNA), a chemical inhibitor of dynein, to block dynein-mediated transport [34-36] and observed a dose-dependent reduction in aggresome formation in cells overexpressing both RFP-G $\beta$ 2 and GFP-Nudel (Figure 3E).

#### *The aggresome formation of G $\beta$ 2 requires the interaction of Nudel with dynein*

We further clarified whether the interaction between Nudel and dynein is important for the aggresome formation of G $\beta$ . To do so, we made use of the mutant Nudel<sup>N20/C36</sup>, which cannot interact with either Lis1 or dynein and thus fails to affect dynein function upon overexpression [19]. Co-IP showed that Flag-Nudel<sup>N20/C36</sup> still associated with G $\beta$ , though with reduced affinity as compared with Flag-Nudel (Figure 4A, lane 6 vs 5). When GFP-Nudel<sup>N20/C36</sup> was overexpressed with RFP-G $\beta$ 2, it failed to facilitate aggresome formation (Figure 4B). These results confirmed that Nudel recruited G $\beta$  to dynein.

Tctex1, a dynein light chain, is known to associate with G $\beta\gamma$  [37]. If dynein could transport G $\beta\gamma$  to the centrosome, overexpression of Tctex1 with G $\beta$  might also form aggresomes. Nevertheless, when Flag-tagged Nudel or Tctex1 was overexpressed with RFP-G $\beta$ 2, only Flag-Nudel stimulated aggresome formation (Figure 4C). Such a result further supports the idea that the G $\beta$ -containing aggresome is formed by mfG $\beta$ , not G $\beta\gamma$ .

#### *Endogenous mfG $\beta$ is enriched in aggresomes upon inhibition of the proteasome activity*

Many proteins are disposed into aggresomes upon inhibition of their proteasome-mediated degradation [12,

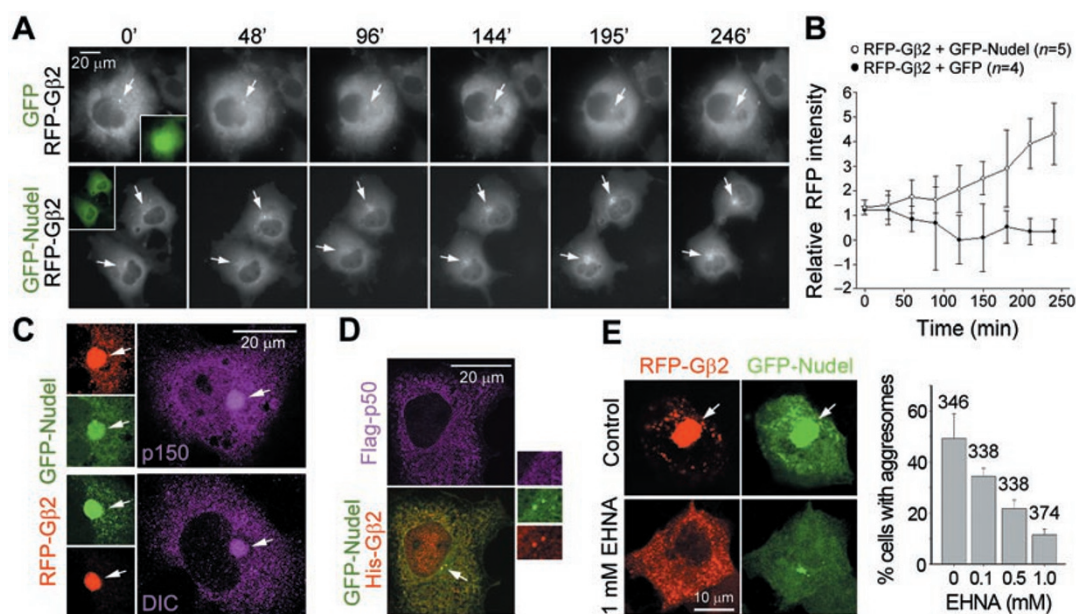


**Figure 3** The formation of the G $\beta$ 2 aggregates requires the dynein-mediated transport. **(A)** The representative RFP image sequences for COS-7 cells overexpressing the indicated proteins. The insets show the expression of GFP or GFP-Nudel. Cells were imaged at 3-min intervals for at least 240 min at 12 h post transfection. The arrows indicate the centrosome regions. **(B)** The statistical analysis for relative RFP intensities at the centrosome regions. The quantification was performed using the images with 30-min intervals. The relative intensity was obtained by normalizing the centrosome/aggresome intensity with the total cell intensity to reduce the influences of quenching or the protein level changes during the imaging. **(C)** The enrichment of dynactin and dynein in the G $\beta$ 2 aggregates. COS-7 cells overexpressing GFP-Nudel and RFP-G $\beta$ 2 were subjected to immunostaining to visualize p150<sup>Glued</sup> or DIC. DIC was detected with the mAb 70.1. The arrows indicate the aggregates. **(D)** Overexpressing p50 abolished the G $\beta$  aggregates formation. COS-7 cells were co-transfected for 48 h to overexpress the indicated proteins. The immunostaining was performed using antibodies to Flag and polyhistidine (His). Centrosome regions that were magnified 2 $\times$  are also shown. **(E)** The dynein inhibitor EHNA repressed the G $\beta$  aggregates formation. The HEK293T cells were transfected to overexpress GFP-Nudel and RFP-G $\beta$ 2 for 24 h and treated with EHNA for another 24 h prior to fixation. The statistical results for the aggregates formation were from two independent experiments. The total numbers of counted cells are listed above the histograms.

13]. To understand whether endogenous G $\beta$  could accumulate in such aggregates, we treated COS-7 cells for 8 h with MG132, a proteasome inhibitor, to induce aggregate formation [38]. In contrast to mock-treated cells, aggregates formed in MG132-treated cells, as indicated by the appearance of cage-like structures of vimentin (Figure 5A, panel 4 vs 2) [12, 32]. G $\beta$  was enriched in these aggregates (Figure 5A, panel 3, arrowheads) compared to its punctate centrosomal localization in mock-treated cells (panel 1, arrowheads). Such data suggest that endogenous G $\beta$  is degraded by the proteasome in cells.

#### *MfG $\beta$ is degraded via the UPS pathway*

We next examined whether G $\beta$  was subjected to polyubiquitination prior to degradation. HEK293T cells were treated with MG132 for 24 h, lysed in the RIPA buffer to disrupt protein-protein interactions, and subjected to IP

using an anti-G $\beta$  antibody (Figure 5B, lanes 1-4; Supplementary information, Figure S6). Compared to the mock-treated cells, the ubiquitination levels of endogenous G $\beta$  markedly increased after MG132 treatment (Figure 5B, lanes 5-6; Supplementary information, Figure S6). When G $\beta$ 1, G $\beta$ 2, G $\beta$ 4, and G $\beta$ 5 were ectopically expressed, polyubiquitination was observed for all of the G $\beta$  isoforms (Supplementary information, Figure S7, lanes 7-10). Moreover, the overexpression significantly increased the ubiquitination levels of the G $\beta$  because polyubiquitinated G $\beta$  was detected in the absence of MG132 (Figure 5C, lane 5 vs 4; Supplementary information, Figure S7). Further overexpression of Gr $\gamma$ 2 to assist the proper folding of excess G $\beta$  [2, 3, 8] largely reduced the ubiquitination levels of exogenous G $\beta$ 2 (Figure 5C, lane 6 vs 5), again suggesting that the polyubiquitination occurs to mfG $\beta$ . Consistently, when Flag-Nudel was used to immunoprecipitate mfG $\beta$ , Nudel-associated G $\beta$  was re-

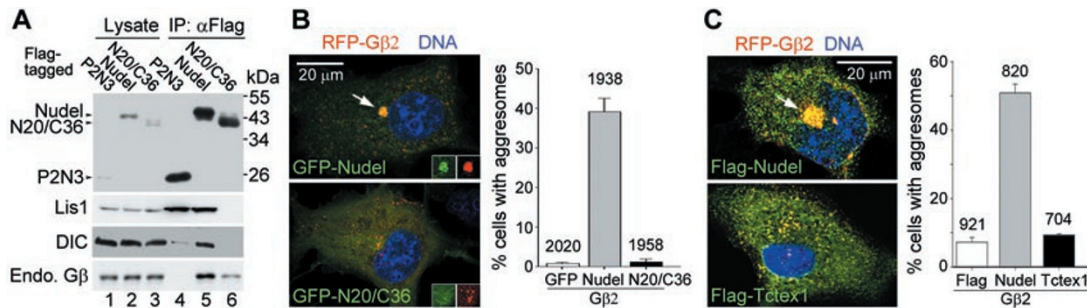


**Figure 4** The formation of the Gβ2 aggregates requires the Nudel-dynein association. **(A)** The association of endogenous Gβ with Nudel<sup>N20/C36</sup>. HEK293T cells overexpressing Flag-tagged Nudel or Nudel mutants were lysed in co-IP buffer and subjected to IP. IB was then performed to detect the indicated proteins. DIC was detected with the mAb 70.1. **(B, C)** The effect of Nudel<sup>N20/C36</sup> or Tctex1 on the aggregate formation of RFP-Gβ2. The COS-7 cells were transfected to co-overexpress the indicated fusion proteins. The arrow points to an aggregate. The insets in **B** show the fluorescence patterns of each protein at the centrosome regions. The statistical results for the aggregate formation were from two independent experiments. The total numbers of cells are listed above histograms.

duced by 50.0% on average in cells overexpressing Gγ2 (Figure 5D, lane 6 vs 5). Interestingly, in contrast to the situation of the Gβ overexpression (Figure 5D), the overexpressed Gγ2 had little effect on the levels of Nudel-associated endogenous mfGβ (Figure 5E, lane 6 vs 7), suggesting that the majority of endogenous mfGβ is probably no longer reversible to the native conformation and is thus destined for degradation.

*Nudel can associate with ubiquitinated Gβ*

We then performed double IP experiments to examine whether Nudel could interact with ubiquitinated Gβ (Figure 5F and 5G). We overexpressed His-Gβ2 in HEK293T cells to enrich the polyubiquitinated Gβ (Figure 5C) and then mixed the cell lysate with those containing Flag-tagged Nudel, Nudel<sup>P2N3</sup>, or Gγ2. Co-IP was then performed using anti-Flag M2 resin to precipitate associated proteins. As expected, Gβ co-immunoprecipitated with both Flag-Nudel (Figure 5G, lane 2) and Flag-Gγ2 (lane 3), but not Flag-Nudel<sup>P2N3</sup> (lane 1). When the immunocomplexes were diluted in the RIPA buffer and subjected to the second round of IP with an anti-Gβ antibody to isolate Gβ, we found that polyubiquitinated Gβ was highly enriched in the immunoprecipitates of Flag-Nudel (Figure 5G, lane 5) compared to those of Flag-Gγ2 (lane 6). Therefore, Nudel is able to interact with both unubiquitinated and ubiquitinated mfGβ (Figure 5F and 5G, lane 5).

*MfGβ associates with dynein in a Nudel-dependent manner*

To further confirm that mfGβ was loaded onto dynein, we examined whether endogenous Gβ was able to associate with dynein. We found that overexpressing low levels of Flag-GFP-DIC2 in HEK293T cells using an internal

ribosome entry site (IRES) [39] followed by co-IP with anti-Flag M2 resin efficiently isolated dynein (marked by DHC and DIC), dynactin (marked by p150<sup>Glu</sup>), and Nudel (Figure 6A and Supplementary information, Figure S8, lane 7). Endogenous Gβ was detected in association with Flag-GFP-DIC2 as well (Figure 6A, lane 3). In contrast, Flag-GFP-p50 expressed in the similar way mainly precipitated dynactin (Supplementary information, Figure S8, lane 6), whereas co-IP with anti-DIC antibody (74.1) only enriched dynein (lane 9) presumably due to disruption of the DIC-p150<sup>Glu</sup> and DIC-Nudel interactions [40, 41]. We thus used Flag-GFP-DIC2 in the following experiments.

First, we examined whether reducing the levels of mfGβ could affect dynein-associated Gβ. Since endogenous mfGβ was hardly restored by extra Gγ2 (Figure 5E), possibly due to fetal structural defects, we overexpressed His-Gβ2 to induce restorable mfGβ (Figures 2D and 5D). Co-IP with anti-Flag resin followed by IB indicated that dynein-associated Gβ decreased in the presence of exogenous Gγ2 (Figure 6B, lane 8 vs 7). Gγ2 itself, however, did not associate with dynein (Figure 6B, lane 8), again suggesting an association of mfGβ, but not the Gβγ dimer, with dynein.

Next, we investigated how Nudel levels impacted the dynein-Gβ interaction. We increased the total levels of Nudel by 5.7±0.6-fold via overexpression of HA-Nudel (Figure 6C, lane 3 vs 2) and found an increased associations of Gβ (by 2.4-fold on average) and Nudel with dynein in co-IP experiments (Figure 6C, lane 8 vs 7). Conversely, knockdown of Nudel expression by RNAi (Figure 6C, lane 5 vs 4) attenuated dynein-associated Gβ (lane 10 vs 9). These data confirm that the Gβ-dynein interaction depends on Nudel.



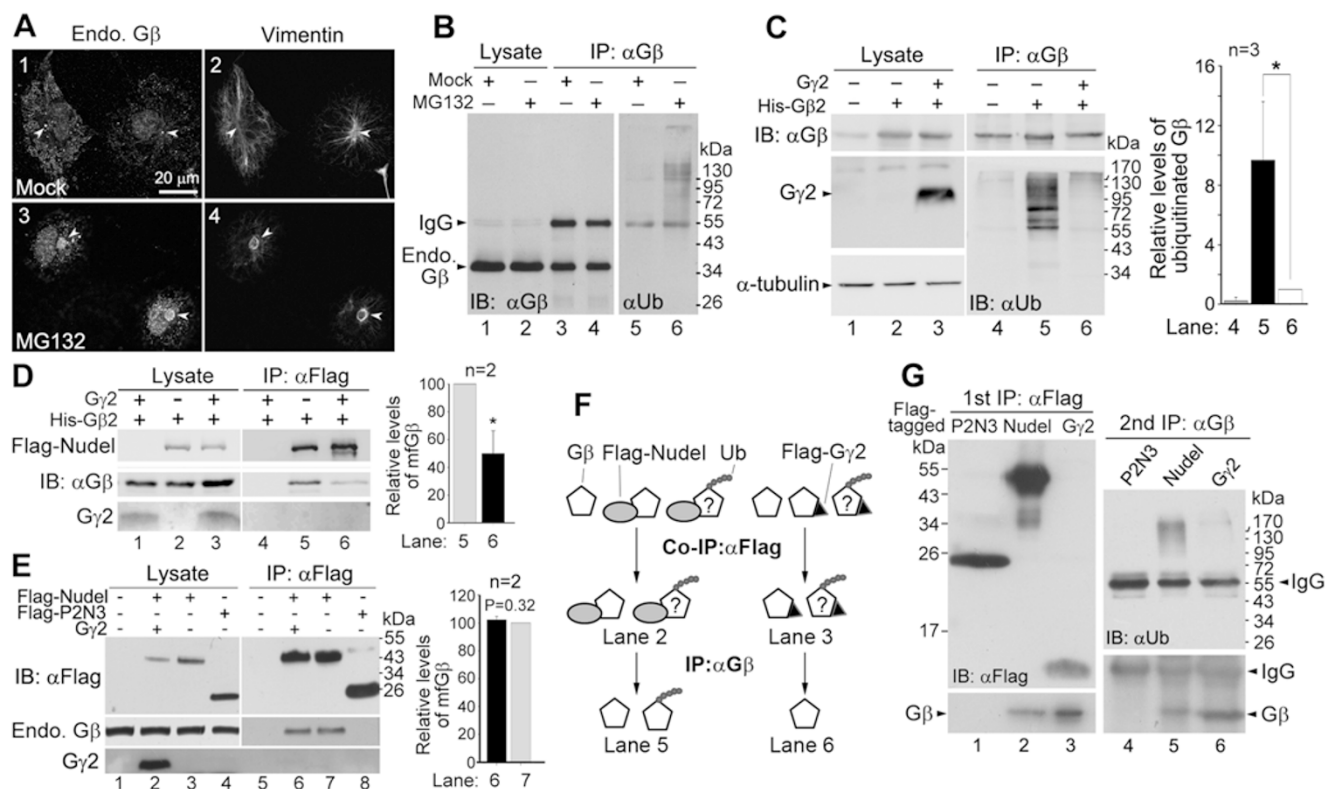


**Figure 5** mFGβ can be ubiquitinated and then degraded through the UPS pathway. **(A)** Endogenous (endo) Gβ was enriched in the aggresomes after the inhibition of proteasome activity. The COS-7 cells treated with MG132 (5 μM) or solvent (DMSO) for 8 h were immunostained to visualize Gβ and vimentin. The arrowheads point to the centrosome regions. **(B)** Endogenous Gβ was able to be polyubiquitinated. The HEK293T cells were treated with MG132 (5 μM) or DMSO for 24 h (lanes 1–2), lysed in the RIPA buffer, and subjected to IP using an anti-Gβ antibody. The IB was then performed using an antibody against either Gβ (lanes 3–4) or Ub (lanes 5–6). **(C)** Exogenous Gβ2 exhibited misfolding-dependent ubiquitination. HEK293T cells were either untransfected (lane 1) or transfected for 48 h to overexpress Gγ2 and/or His-Gβ2 (lanes 2–3). The cells were lysed in the RIPA buffer and subjected to IP using an anti-Gβ antibody. The histogram shows the quantification results of three independent experiments. The intensities of the ubiquitinated Gβ were normalized with those of corresponding Gβ. \*indicates  $P < 0.05$  in Student's  $t$ -test. **(D, E)** The effect of Gγ2 overexpression on the Gβ-Nudel interaction. HEK293T cells overexpressing the indicated proteins were subjected to co-IP using anti-Flag M2 resin. The band intensities of Gβ were normalized with those of corresponding Flag-Nudel and are presented in histograms. **(F, G)** Ubiquitinated Gβ was able to associate with Nudel. Approximately  $1 \times 10^8$  HEK293T cells overexpressing His-Gβ2 were lysed in the co-IP buffer, mixed with an equal amount of lysate containing Flag-tagged Nudel, Nudel<sup>P2N3</sup>, or Gγ2, respectively, and co-immunoprecipitated using anti-Flag M2 resin (lanes 1–3). The immunocomplexes were then diluted in the RIPA buffer and subjected to the second round of IP using an anti-Gβ antibody (lanes 4–6). The experiments are diagrammed in **F**.

### Dynein-mediated transport promotes the degradation of mFGβ

To confirm that endogenous mFGβ was indeed transported to the centrosome in dynein and Nudel-dependent manner, we knocked down Nudel in HeLa cells using three different siRNAs (Figure 7A), which was expected to both inactivate dynein-mediated protein transport [22, 31] and prevent mFGβ from loading onto dynein (Figures 5 and 6). To facilitate the detection of mFGβ, we treated cells with MG132 for 12 h to increase the levels of endogenous polyubiquitinated mFGβ (Figure 5A and 5B)

and performed immunostaining (Figure 7B). Similar to untransfected cells (Figure 5A), aggresome formation was observed in 39.6% of cells transfected with control oligo on average (Figure 7B and 7C). By contrast, aggresomes were seen in only 2.4%–8.8% of cells after the depletion of Nudel (Figure 7B and 7C).

To understand whether the dynein-mediated transport affects Gβ turnover, we compared the half-life of nascent Gβ in control or Nudel RNAi cells. When nascent Gβ in control cells was pulse-labeled with <sup>35</sup>S-Met/Cys and then chased for up to 3 h, its half-life was estimated to



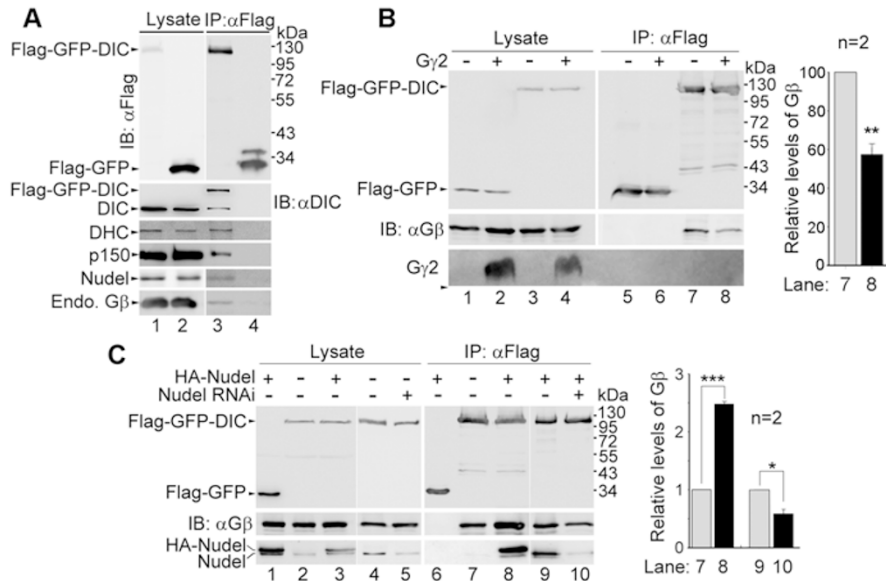


**Figure 6** mfGβ associates with dynein in a Nudel-dependent way. **(A)** The association of endogenous Gβ with dynein. The HEK293T cells overexpressing Flag-GFP-DIC or Flag-GFP were subjected to co-IP using anti-Flag M2 resin. IB was then performed to detect the indicated proteins. Please note that Flag-GFP-DIC was not detected in the lysate with the antibody to DIC due to its low levels (lane 1), unless the blot was overexposed (data not shown). **(B)** Decreasing the levels of mfGβ by overexpression of Gγ2 reduced the Gβ-dynein association. HEK293T cells overexpressing His-Gβ2 and the indicated proteins were subjected to co-IP using anti-Flag M2 resin. \*\*indicates  $P < 0.01$  in Student's  $t$ -test. **(C)** The Gβ-dynein association depended on Nudel. HEK293T cells were transfected to overexpress His-Gβ2 and the indicated tagged proteins or to knock down Nudel by RNAi. Co-IP was then performed using anti-Flag M2 resin. \* and \*\*\* indicates  $P < 0.05$  and  $0.001$ , respectively.

be ~0.8 h (Figure 7D-7F). However, in Nudel-depleted cells, the protein was markedly stabilized, with a half-life of more than 3 h (Figure 7D-7F). Therefore, the dynein-mediated transport of Gβ mainly facilitates the degradation of Gβ.

*Long-term activation of Gβγ signaling increases Gβ ubiquitination*

To assess whether proteasome-mediated degradation could serve as negative feedback to quench Gβγ signaling, we traced ubiquitination levels of Gβ after the activation of a typical GPCR, β2-adrenergic receptor (β2AR). We initially treated HEK293T cells with isoproterenol (Iso), a βAR agonist [42], for 10 h in the presence of MG132, but we failed to see a clear change in Gβ ubiquitination levels. We thus overexpressed HA-β2AR (Figure 8A, lane 2) to enhance the cellular response to Iso stimulation. In cells overexpressing HA-β2AR, Iso induced ERK1/2 activation as well as an accumulation of the polyubiquitinated Gβ (Figure 8A, lane 2 vs 1).

We then tested whether the activation of Gβγ in a GPCR-independent manner could also promote Gβ ubiquitination. HEK293T cells were transfected to overexpress Flag-tagged LGN to activate Gβγ signaling in a GPCR-

independent manner [5]. Cells were collected at 10, 20, or 30 h post transfection to achieve different LGN expression levels (Figure 8B, lanes 2-4). To enrich ubiquitinated Gβ, cells were also treated with MG132 for 10 h prior to lysis with the RIPA buffer. IP with an anti-Gβ antibody indicated that the ubiquitinated Gβ positively correlated with LGN levels (Figure 8B, lanes 1-4). These data indicate that the sustained activation of Gβγ signaling is accompanied by the elevated ubiquitination of Gβ.

**Discussion**

*Nudel selectively interacts with mfGβ*

We showed that Nudel distinguishes itself from all other known Gβ-interacting proteins [1, 4] in that it only interacts with Gγ-free Gβ, which is generally believed to be unfolded or misfolded [2, 3, 8]. First, Nudel associated with Gγ-free Gβ both *in vitro* and *in vivo* (Figures 1, 5D and 5E). In addition to the full-length Gβ, Nudel also associated with deletion mutants of Gβ2 that contained only portions of the seven WD repeats (Figure 1). Second, Nudel was able to interact with polyubiquitinated Gβ (Figure 5F and 5G). Such forms of Gβ are most likely misfolded because they were enriched after the MG132

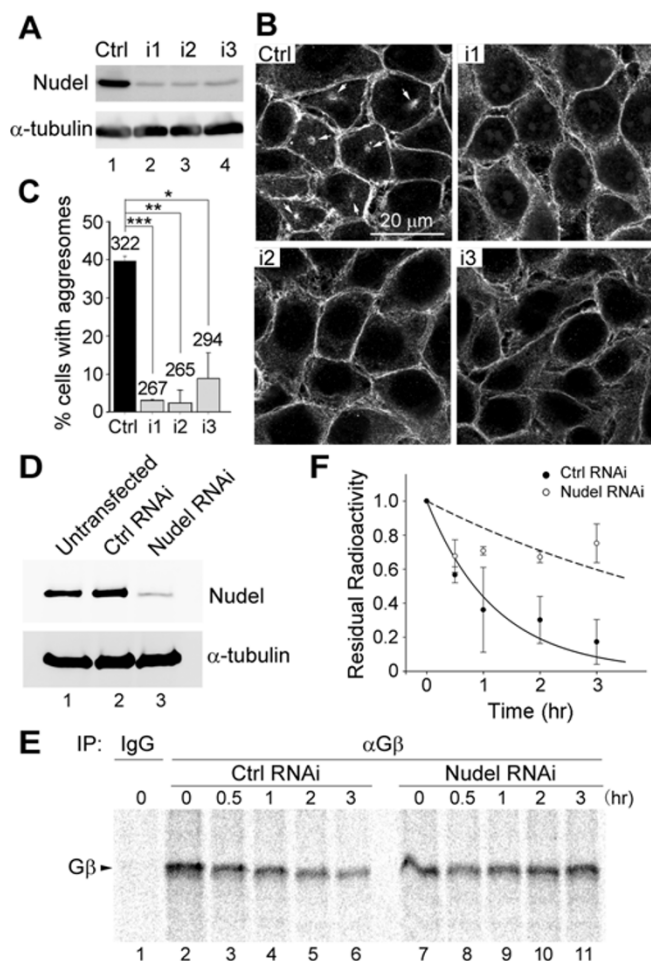


**Figure 7** Nudel RNAi impairs the centrosomal accumulation of mfG $\beta$  and its turnover. **(A)** Confirmation of the Nudel RNAi efficiencies of individual siRNAs by IB. HeLa cells were transfected with a control oligo or one of the three siRNAs (i1-i3) for 72 h. **(B, C)** Nudel RNAi impaired the centrosomal accumulation of endogenous mfG $\beta$ . HeLa cells transfected with the indicated oligos for 60 h were treated with MG132 (5 mM) for 12 h prior to the fixation. Immunostaining was then performed with an anti-G $\beta$  antibody. The statistical data were obtained from two independent experiments. The total numbers of cells are listed above the histograms. **(D)** Nudel RNAi efficiency in pulse-chase experiments. HEK293T cells were transfected with the control oligo or a mixture of i1-i3 for 48 h. A set of sample was then collected for IB. **(E, F)** Nudel RNAi markedly stabilized nascent G $\beta$ . Cells transfected with siRNAs for 48 h were pulse-labeled with  $^{35}\text{S}$ -Met/Cys for 1 h and then chased for the indicated time. G $\beta$  was immunoprecipitated with anti-G $\beta$  antibody and subjected to SDS-PAGE and autoradiography. Its relative radioactivity was averaged from the results of two independent experiments. The curve fitting of the pulse chase data was performed using SigmaPlot.

treatment and were accumulated in the aggresome for degradation and sequestration (Figures 2C, 5B and 5C). Third, the aggresome formed by the overexpression of

both G $\beta$ 2 and Nudel was devoid of G $\gamma$ 2 (Figure 2C). This piece of data further confirmed the interaction between the G $\gamma$ -free G $\beta$  and Nudel. Finally, the amount of Nudel-associated G $\beta$  is positively correlated with the levels of G $\gamma$ -free G $\beta$ . Overexpression of G $\beta$ 2 only slightly increased the total steady-state levels of G $\beta$  but dramatically stimulated the Nudel-G $\beta$  interaction (Figure 2D). Such a phenomenon is attributed to the marked increase in mfG $\beta$  levels, as judged by the robust polyubiquitination of G $\beta$  (Figure 5C). The overexpression of G $\gamma$ 2 attenuated the levels of both polyubiquitinated and Nudel-associated G $\beta$  (Figure 5C and 5D). Interestingly, we found that overexpressed G $\gamma$ 2 was unable to strongly attenuate the levels of endogenous mfG $\beta$  (Figure 5E), possibly because such mfG $\beta$  was already destined for degradation and thus irreversible to the native conformation. It should be noted that, although the overexpression of G $\beta$ 2 markedly elevated the levels of mfG $\beta$  (Figure 2D, lane 6 vs 5; Figure 5C, lane 5 vs 6), possibly due to increased nascent G $\beta$  over endogenous G $\gamma$ , the overexpression only led to a mild increase in the total levels of G $\beta$  (Figure 2D, lane 3 vs 2; Figure 5C, lanes 2-3 vs 1; Supplementary information, Figure S7, lanes 2-5 vs 1). Thus, we used the overexpression to increase the levels of mfG $\beta$  in this study to facilitate the biochemical and cytological assays. We also confirmed our major results with endogenous proteins.

Domain mapping suggests that Nudel uses its N-terminal region to bind to the WD repeats of G $\beta$  (Figure 1E, 1F and Supplementary information, Figure S2). Interestingly, Nudel contains the “QXXER” motif that is found in many G $\beta$  $\gamma$  effectors [27]. A peptide from AC2 that covers this motif can bind to multiple regions in the WD repeats of G $\beta$ 1 [27, 28]. Since this motif also contributes to the Nudel-G $\beta$  interaction (Figure 1 and Supplementary information, Figure S2), it may mediate the interaction of Nudel with the WD repeats of G $\beta$  as well.

#### *Dynein transports Nudel-associated mfG $\beta$ to the centrosome for degradation*

Our results suggested that mfG $\beta$  is subjected to dynein-mediated transport to the centrosome (Figure 8C). Dynein associated with G $\gamma$ -free G $\beta$  (Figure 6B). Reducing the levels of mfG $\beta$  by overexpressing G $\gamma$ 2 attenuated the levels of dynein-associated G $\beta$  (Figure 6A and 6B). More importantly, inhibition of dynein activity by either p50 overexpression or EHNA treatment repressed the aggresome formation of mfG $\beta$ 2 (Figure 3). The knock-down of Nudel by RNAi also disrupted the aggresome formation of endogenous mfG $\beta$  (Figure 7A-7C), though depletion of Nudel may impair both the dynein activity [22, 31] and the loading of G $\beta$  onto dynein (see below).

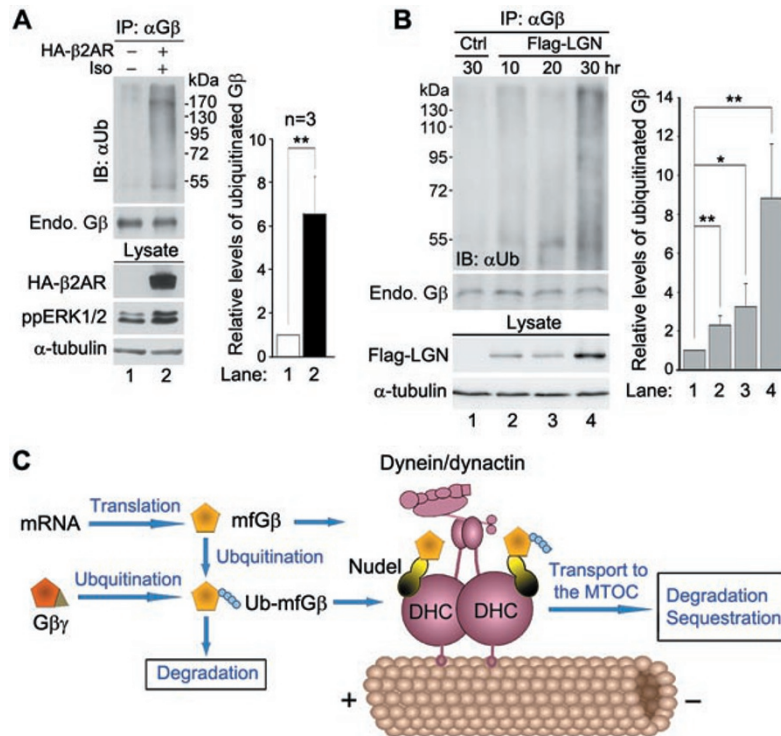


**Figure 8** The polyubiquitination of Gβ can be stimulated through the sustained activation of Gβγ signaling. **(A)** The activation of Gβγ signaling via β2AR. HEK293T cells transfected for 38 h to overexpress HA-β2AR were treated with Iso and MG132 for an additional 10 h (lane 2), whereas the mock-transfected cells were treated only with MG132 (lane 1). The cells were then lysed in the RIPA buffer. The activation of Gβγ signaling was assessed by the increase in phosphorylated ERK1/2 (lane 2 vs 1). The lysates were subjected to IP using an anti-Gβ antibody (lanes 3-4). The intensities of ubiquitinated Gβ were normalized with those of the corresponding Gβ. **(B)** The activation of Gβγ signaling via LGN. Flag-LGN was overexpressed in HEK293T cells to induce the dissociation of Gβγ from Gα. The transfected cells were collected at the indicated time points after MG132 treatment for 10 h. The cell lysates in the RIPA buffer (lanes 1-4) were subjected to IP using an anti-Gβ antibody (lanes 5-8). The histograms show the quantification results of three independent experiments. **(C)** A model for the role of Nudel in the disposal of mfGβ. mfGβ may be generated after either the translation or the Gβγ signaling. It may either be degraded in the cytoplasm or be recruited to dynein by Nudel, followed by the transport to the MTOC for degradation and sequestration.

The failure of Tctex1 [37] overexpression to promote the formation of Gβ-containing aggresomes further suggests that dynein transports mfGβ, not Gβγ (Figure 4C).

We demonstrated that Nudel mediates the mfGβ-dynein association (Figure 8C). Dynein activity at basal levels is already sufficient for aggresome formation because mutant cystic fibrosis transmembrane regulator (CFTR<sup>F508</sup>) or GFP-250 alone can form aggresomes upon overexpression [32, 43]. The overexpressed Gβ2 or its WD repeat-containing mutant Gβ2C also formed the aggresome-like structures in a fraction of cells (Figure 2F). Therefore, the positive effect of the Nudel overexpression on the Gβ aggresome formation (Figure 2 and Supplementary information, Figure S4) is attributed to a more efficient loading of mfGβ onto dynein due to the increased Nudel-mfGβ interaction (Figure 2). Consistently, the levels of dynein-associated mfGβ (Figure 6B)

were correlated with Nudel levels in the co-IP experiments (Figure 6C). The aggresome formation was independent of the expression tags that were used for the expressions of the exogenous Gβ and Nudel. Besides, GFP or GFP-Gβ2N, which was incapable of binding Nudel, failed to form the aggresomes regardless of the Nudel levels (Figure 2E and 2F), indicating the specificity of the aggresome formation. Specifically blocking the loading of mfGβ onto dynein through the overexpression of Nudel<sup>N20/C36</sup>, a Nudel mutant that was able to interact with Gβ but not dynein (Figure 4A) [19, 22], also repressed the aggresome formation of the overexpressed Gβ2 (Figure 4B). The knockdown of Nudel by RNAi abolished the Gβ-dynein association as well (Figure 6C).

The centrosome is thought to be a site of protein sequestration, degradation, and refolding [44-46]. Since the half-life of nascent Gβ was markedly prolonged in cells



deprived of Nudel (Figure 7D and 7F), we concluded that mfG $\beta$  is transported to the MTOC for degradation (Figure 8C). The centrosomal localization of endogenous G $\beta$  in intact cells (Supplementary information, Figure S3B) may reflect the steady-state levels of mfG $\beta$ , as a result of the dynamic balance between its accumulation and degradation. When the dynein-mediated transport of mfG $\beta$  surpasses the protein degradation rate at the centrosome, as in the case of MG132 treatment (Figure 5A) or G $\beta$  overexpression (Figure 2 and Supplementary information, Figure S4), the accumulated misfolded protein(s) then trigger the aggresome formation and is thus sequestered from the cytosol. Interestingly, G $\beta$ 2 has recently been shown to exhibit a G $\gamma$ -independent function in mitochondrial fusion via the interaction with mitofusin 1 [47]. Whether this unique function of G $\beta$ 2 requires its dynein-mediated transport, however, is currently not known.

#### *Degradation of mfG $\beta$ is important for the protein quality control and possibly the negative regulation of G $\beta\gamma$ signaling*

Like many other proteins [11], mfG $\beta$ , possibly resulting from translational errors [11] or the failure to form a G $\beta\gamma$  dimer [4, 8], is also a target of the cellular protein quality control machinery and is thus subjected to degradation by the UPS system (Figure 8C). Overexpression of G $\beta$  markedly increased the levels of mfG $\beta$  (Figure 2D) and of polyubiquitinated G $\beta$  (Figure 5C and Supplementary information, Figure S7). The existence of Nudel-associated endogenous G $\beta$  that was free of G $\gamma$ 2 (Figures 1C, 1D, 2D and 5E) indicates the presence of mfG $\beta$  in intact cells. The enrichment of polyubiquitinated G $\beta$  after the MG132 treatment (Figure 5B) indicates that the proteasome-mediated degradation of the protein occurs as a constitutive process in cells.

Emerging lines of evidence suggest that the degradation of G $\beta$  is also used to negatively regulate G $\beta\gamma$  signaling. Excess G $\beta\gamma$  results in increased G $\beta$  degradation [10]. Chronic stimulation of a GPCR leads to G $\beta$  degradation as well [9]. We found that long-term activation of G $\beta\gamma$  signaling through either a GPCR ( $\beta$ 2AR) or LGN increased the levels of polyubiquitinated G $\beta$  (Figure 8A and 8B). These results strongly suggest the existence of a cellular mechanism to prevent excessive G $\beta\gamma$  signaling by degrading G $\beta$  (Figure 8C). Such a negative feedback mechanism could apparently provide more precise control over G $\beta\gamma$  signaling, though further investigation is needed for a more detailed understanding of the mechanism. In addition to the G $\beta\gamma$  signaling, the functions of AGS family may also be regulated by the aggresome pathway because Gai has been shown to prevent the ag-

gresome localization of AGS3 promoted by Inscuteable or MG132 [7].

Because the proteasome-mediated degradation can occur both in the cytosol and at the centrosome [11, 44, 46], the dynein-mediated transport appears to function to efficiently clear mfG $\beta$  from the cytosol, allowing its rapid sequestration and degradation at the centrosome to possibly reduce the deleterious effects of misfolded proteins in the cytosol [12, 48]. Interestingly, in addition to G $\beta$ , the Nudel-binding proteins Lis1 and DIC are also WD repeat-containing proteins [16, 29, 41]. Thus, Nudel might bind other WD-repeat proteins as well to either carry out physiological functions (similar to Lis1 and DIC) or promote the clearance of their misfolded forms (like G $\beta$ ).

## Materials and Methods

### *Plasmids and siRNAs*

The expression plasmids for Flag or GFP-tagged p50 (dynamin), human Nudel and its mutants, Nudel<sup>C36</sup>, Nudel<sup>N20/C36</sup>, and Nudel<sup>P2N</sup>, were described previously [19, 22, 30]. Other deletion or point mutants of Nudel described in this study were generated by polymerase-chain reaction (PCR). pEGFP-C1 (Clontech) was used to express GFP-G $\beta$ 2 or its mutants, whereas RFP-G $\beta$ 2 was expressed using a modified vector [22]. His- or HA-tagged G $\beta$ 2 was expressed using pcDNA3 (Invitrogen). HA-tagged G $\beta$ 1, G $\beta$ 4, and G $\beta$ 5, whose cDNAs were kindly provided by Dr N Gautam (Washington University at St. Louis, USA), were expressed using pcDNA3. pcDNA3-G $\gamma$ 2 from Dr P Wedegaertner (Thomas Jefferson University, USA) was used to amplify the G $\gamma$ 2 cDNA for construction of a Flag-G $\gamma$ 2-expression plasmid using pUHD30F [49]. pXJ40-Flag-LGN was kindly provided by Dr S Bahri (Institute of Molecular and Cell Biology, Singapore). The expression plasmids for HA- $\beta$ 2AR and Flag-Tctex1 were from Drs G Pei and S Yang, respectively (Institute of Biochemistry and Cell Biology, China). pLV-IRES-Flag-GFP was described previously [39] and was used to construct pLV-IRES-Flag-GFP-DIC2 to express low levels of mouse DIC2. pFlag1 (IBI) and pTrc-HisA (Invitrogen) were used to express Flag- or His-tagged proteins in *E. coli*. All the PCR-amplified DNA sequences were verified by sequencing.

The siRNAs against human Nudel mRNA were purchased from Invitrogen. Their sequences are 5'-GAGCAUCAUAUG-CACAGAGCUAUA-3'; 5'-GGUCUCAGUGUUAGAAGAU-GAUUUA-3'; and 5'-CCAGGCCAUUGAACGAAAUG-CAUUU-3'.

### *Antibodies and reagents*

Mouse monoclonal antibodies to  $\alpha$ -tubulin,  $\gamma$ -tubulin, DIC (70.1), and to Flag, HA, and His tags were purchased from Sigma. Mouse monoclonal antibodies to p150<sup>Glued</sup> and DIC (74.1) were from BD Biosciences and Chemicon, respectively. Mouse antibody to ninein was kindly provided by G Chan (University of Alberta, Canada). Rabbit anti-phospho-Erk1/2 (Thr202/Tyr204) antibody was purchased from Cell Signaling Technology. Rabbit antibodies to GFP, Ub, DHC, Gai, Gas, G $\gamma$ 2, and pan-G $\beta$  were from Santa Cruz Biotechnology. Rabbit antibodies to the Flag tag

and  $\gamma$ -tubulin were from Sigma. Goat polyclonal antibody to LGN (also named GPSM2) and rabbit polyclonal to LIS1 were from Abcam. Anti-Nudel IgY was generated from chicken [22]. Rabbit polyclonal antibodies to G $\gamma$  and Centrin1 were from ProteinTech Group. Secondary antibodies conjugated with Alexa 405, 488, 546, or 633 were from Molecular Probes. Cy5-conjugated antibodies were from Rockland.

Isoproterenol (Iso), 4',6-diamidino-2-phenylindole (DAPI), EHNA, and MG132 were purchased from Sigma.

#### Yeast two-hybrid screen

The MATCHMAKER GAL4 two-hybrid system 2 and a human placenta cDNA library in pACT2 were from Clontech. Human Nudel was expressed using pAS2-1 as the bait. The screening was performed following the manufacturer's manuals.

#### Cell culture and transfection

HEK293T, COS-7, or HeLa cells were cultured in Dulbecco's modified Eagle's medium (Invitrogen) containing 10% bovine serum (Sijiqing Company, Hangzhou, China) in 5% CO<sub>2</sub> at 37 °C. The plasmid transfection was performed using the conventional calcium phosphate method, whereas the siRNAs were transfected using Lipofectamine 2000 (Invitrogen). In overexpression experiments, the cells were harvested approximately 48 h post transfection for biochemical assays or fixed for microscopy unless otherwise described. Usually, HEK293T cells were used for the biochemical assays due to their high transfection efficiency, while COS-7 and HeLa cells were used for the microscopic analyses due to their large cell sizes.

#### Fluorescence microscopy

Generally, cells grown on coverslip were fixed in 4% paraformaldehyde for 15 min and then permeabilized with either 0.5% Triton X-100 in PBS or cold methanol for 5 min prior to immunofluorescence staining. Proper antibody combinations were chosen for multi-color staining, whereas fluorescent proteins were visualized via their autofluorescence. Nuclear DNA was stained with DAPI. To stain for endogenous centrosomal G $\beta$ , cells were permeabilized with 0.1% Triton X-100 in PEM buffer (80 mM PIPES at pH 6.9, 1 mM EGTA, 1 mM MgCl<sub>2</sub>) for 1 min, followed by fixation in PEM buffer containing 4% paraformaldehyde. Fluorescence images were captured by using an Olympus BX51 microscope with a cold CCD camera (SPOT II, Diagnostic), or a laser confocal microscope (Leica TCS SP2 or SP5). For confocal microscopy with fixed cells, optical sections were scanned at 0.1-0.5  $\mu$ m intervals. Z stack images were then formed by maximal projection.

For live-cell imaging, pEGFP-C1 (Clontech) or pEGFP-Nudel was cotransfected with pRFP-G $\beta$ 2 at 1:1 ratio into COS-7 cells. Cells were imaged at 37 °C using Leica AS MDW microscope system equipped with a cool CCD camera (SNAP HQ, Roper Scientific).

Quantitation for fluorescence intensities was done as described [50] with minor modifications. Statistic results were obtained in a blind fashion and presented as mean  $\pm$  SD.

#### Immunoprecipitation and immunoblotting

For immunoprecipitation (IP) of protein complexes, HEK293T cells were lysed in co-IP buffer (20 mM Tris-Cl, pH 7.4, 150 mM KCl, 1 mM EDTA, 50 mM NaF, 1 mM DTT, 1% NP-40,

10% glycerol, and 10 mM sodium pyrophosphate, together with protease inhibitors). For IP of the target protein alone, cells were lysed in the RIPA buffer (50 mM Tris-HCl, pH 8.0, 150 mM NaCl, 1% NP-40, 0.5% sodium deoxycholate, 0.1% SDS, 5 mM EDTA, 10 mM NaF, 1 mM DTT, together with protease inhibitors). The Flag-tagged proteins were precipitated using anti-Flag M2 resin (Sigma) as described [30]. HA-tagged proteins were precipitated by EZview™ Red Anti-HA Affinity Gel (Sigma) according to the instructions. Other proteins were precipitated using ~2  $\mu$ g of antibody and 25  $\mu$ l 50% slurry of protein G (Invitrogen) or protein A (Pharmacia) Sepharose.

The bacterially expressed proteins were induced by IPTG as described [51]. For *in vitro* binding assay, *E. coli* was lysed in lysis buffer (10 mM Tris-HCl, 150 mM NaCl, 1% NP-40, 10 mM EDTA, 5 mM DTT) by sonication. Flag-tagged proteins expressed in *E. coli* were each immobilized on 20  $\mu$ l of anti-Flag M2 beads (Sigma) and incubated with 400  $\mu$ l of bacterial lysate containing His-G $\beta$ 2 for 2 h at 4 °C. After three times of wash, bound proteins were eluted using Flag peptide.

Proteins were resolved by conventional SDS-PAGE, except that G $\gamma$  was separated with Tris-Tricine-SDS-PAGE [52]. Immunoblots were developed in Western Lightning Chemiluminescence Reagent Plus (PerkinElmer Life and Analytical Sciences) and exposed to X-ray films (Kodak) or with Luminescent Image Analyzer (Fujifilm LAS4000). Blots were stripped for re-probing when necessary.

#### Pulse-chase analysis

Pulse-chase experiments were performed as described [53] with minor modifications. Briefly, HEK293T cells transfected with siRNAs for 48 h and grown in 60-mm Petri dishes were pre-incubated in Dulbecco's modified Eagle's medium minus Met and Cys (Invitrogen) for 1 h. Each plate of cells was then labeled with 1 ml of the medium containing 18  $\mu$ l (200  $\mu$ Ci) of EasyTag™ EXPRESS <sup>35</sup>S Protein Labeling Mix (11 mCi/ml, Perkin Elmer) for 1 h. Cells were rinsed three times with the medium supplemented with 10% of fetal bovine serum and 2 mM of cold Met and Cys (Sigma-Aldrich), chased in the same medium for different time, and lysed in the RIPA buffer. G $\beta$  was immunoprecipitated with anti-G $\beta$  antibody from lysates with equal total radioactivity and subjected to 15% SDS-PAGE. Autoradiography was performed with Fluorescent Image Analyzer (FLA-9000, FujiFilm). Band intensities were quantified with Multi Gauge software (FujiFilm). Dynamic Curve Fitting of the pulse chase data was performed with SigmaPlot software.

#### Acknowledgments

We thank Dr Yixian Zheng (Carnegie Institution for Science, USA) and Dr Ronggui Hu (Institute of Biochemistry and Cell Biology (IBCB), Chinese Academy of Sciences (CAS)) for helpful suggestions and discussions, Qiongping Huang, Wei Yu and Yan Li for technical assistance. We also thank Drs Narasimhan Gautam (Washington University at St. Louis, USA) for G $\beta$  cDNAs, Phillip B Wedegaertner (Thomas Jefferson University, USA) for pcDNA3-G $\gamma$ 2, Sami Bahri (Institute of Molecular and Cell Biology, Singapore) for pXJ40-Flag-LGN, Gordon Chan (University of Alberta, Canada) for the ninein antibody, Gang Pei (IBCB, CAS) for pcDNA3-HA- $\beta$ 2AR, and Shuo Yang (ICBC, CAS) for pFlag-Tctex1. This work was supported by the National Basic Re-

search Program of China (2010CB912102 and 2012CB945003), the National Natural Science Foundation of China (30830060 and 31010103910), Chinese Academy of Sciences (XDA01010107), and Science and Technology Commission of Shanghai Municipality (09JC1416200).

## References

- Smrcka AV. G protein betagamma subunits: central mediators of G protein-coupled receptor signaling. *Cell Mol Life Sci* 2008; **65**:2191-2214.
- Clapham DE, Neer EJ. G protein beta gamma subunits. *Annu Rev Pharmacol Toxicol* 1997; **37**:167-203.
- Gautam N, Downes GB, Yan K, Kisselev O. The G-protein betagamma complex. *Cell Signal* 1998; **10**:447-455.
- Dupre DJ, Robitaille M, Rebois RV, Hebert TE. The role of Gbetagamma subunits in the organization, assembly, and function of GPCR signaling complexes. *Annu Rev Pharmacol Toxicol* 2009; **49**:31-56.
- Blumer JB, Smrcka AV, Lanier SM. Mechanistic pathways and biological roles for receptor-independent activators of G-protein signaling. *Pharmacol Ther* 2007; **113**:488-506.
- Knust E. G protein signaling and asymmetric cell division. *Cell* 2001; **107**:125-128.
- Vural A, Oner S, An N, et al. Distribution of activator of G-protein signaling 3 within the aggresomal pathway: role of specific residues in the tetratricopeptide repeat domain and differential regulation by the AGS3 binding partners Gi(alpha) and mammalian inscuteable. *Mol Cell Biol* 2010; **30**:1528-1540.
- Marrari Y, Crouthamel M, Irannejad R, Wedegaertner PB. Assembly and trafficking of heterotrimeric G proteins. *Biochemistry* 2007; **46**:7665-7677.
- Mouledous L, Neasta J, Uttenweiler-Joseph S, et al. Long-term morphine treatment enhances proteasome-dependent degradation of G beta in human neuroblastoma SH-SY5Y cells: correlation with onset of adenylyl cyclase sensitization. *Mol Pharmacol* 2005; **68**:467-476.
- Lee YI, Kim SY, Cho CH, et al. Coordinate expression of the alpha and beta subunits of heterotrimeric G proteins involves regulation of protein degradation in CHO cells. *FEBS Lett* 2003; **555**:329-334.
- Wickner S, Maurizi MR, Gottesman S. Posttranslational quality control: folding, refolding, and degrading proteins. *Science* 1999; **286**:1888-1893.
- Garcia-Mata R, Gao YS, Sztul E. Hassles with taking out the garbage: aggravating aggresomes. *Traffic* 2002; **3**:388-396.
- Corboy MJ, Thomas PJ, Wigley WC. Aggresome formation. *Methods Mol Biol* 2005; **301**:305-327.
- Olzmann JA, Li L, Chin LS. Aggresome formation and neurodegenerative diseases: therapeutic implications. *Curr Med Chem* 2008; **15**:47-60.
- Hirokawa N. Kinesin and dynein superfamily proteins and the mechanism of organelle transport. *Science* 1998; **279**:519-526.
- Vallee RB, Williams JC, Varma D, Barnhart LE. Dynein: an ancient motor protein involved in multiple modes of transport. *J Neurobiol* 2004; **58**:189-200.
- Li SH, Gutekunst CA, Hersch SM, Li XJ. Interaction of huntingtin-associated protein with dynactin P150Glued. *J Neurosci* 1998; **18**:1261-1269.
- Kawaguchi Y, Kovacs JJ, McLaurin A, Vance JM, Ito A, Yao TP. The deacetylase HDAC6 regulates aggresome formation and cell viability in response to misfolded protein stress. *Cell* 2003; **115**:727-738.
- Liang Y, Yu W, Li Y, et al. Nudel functions in membrane traffic mainly through association with Lis1 and cytoplasmic dynein. *J Cell Biol* 2004; **164**:557-566.
- Shu T, Ayala R, Nguyen MD, Xie Z, Gleeson JG, Tsai LH. Ndel1 operates in a common pathway with LIS1 and cytoplasmic dynein to regulate cortical neuronal positioning. *Neuron* 2004; **44**:263-277.
- Nguyen MD, Shu T, Sanada K, et al. A NUDEL-dependent mechanism of neurofilament assembly regulates the integrity of CNS neurons. *Nat Cell Biol* 2004; **6**:595-608.
- Liang Y, Yu W, Li Y, et al. Nudel modulates kinetochore association and function of cytoplasmic dynein in M phase. *Mol Biol Cell* 2007; **18**:2656-2666.
- Zhang Q, Wang F, Cao J, et al. Nudel promotes axonal lysosome clearance and endo-lysosome formation via dynein-mediated transport. *Traffic* 2009; **10**:1337-1349.
- Li Y, Yu W, Liang Y, Zhu X. Kinetochore dynein generates a poleward pulling force to facilitate congression and full chromosome alignment. *Cell Res* 2007; **17**:701-712.
- Yan K, Kalyanaraman V, Gautam N. Differential ability to form the G protein betagamma complex among members of the beta and gamma subunit families. *J Biol Chem* 1996; **271**:7141-7146.
- Evanko DS, Thiyagarajan MM, Siderovski DP, Wedegaertner PB. Gbeta gamma isoforms selectively rescue plasma membrane localization and palmitoylation of mutant Galphas and Galphaq. *J Biol Chem* 2001; **276**:23945-23953.
- Chen J, DeVivo M, Dingus J, et al. A region of adenylyl cyclase 2 critical for regulation by G protein beta gamma subunits. *Science* 1995; **268**:1166-1169.
- Weng G, Li J, Dingus J, Hildebrandt JD, Weinstein H, Iyengar R. Gbeta subunit interacts with a peptide encoding region 956-982 of adenylyl cyclase 2. Cross-linking of the peptide to free Gbetagamma but not the heterotrimer. *J Biol Chem* 1996; **271**:26445-26448.
- Sasaki S, Shionoya A, Ishida M, et al. A LIS1/NUDEL/cytoplasmic dynein heavy chain complex in the developing and adult nervous system. *Neuron* 2000; **28**:681-696.
- Yan X, Li F, Liang Y, et al. Human Nudel and NudE as regulators of cytoplasmic dynein in poleward protein transport along the mitotic spindle. *Mol Cell Biol* 2003; **23**:1239-1250.
- Guo J, Yang Z, Song W, et al. Nudel contributes to microtubule anchoring at the mother centriole and is involved in both dynein-dependent and -independent centrosomal protein assembly. *Mol Biol Cell* 2006; **17**:680-689.
- Garcia-Mata R, Bebek Z, Sorscher EJ, Sztul ES. Characterization and dynamics of aggresome formation by a cytosolic GFP-chimera. *J Cell Biol* 1999; **146**:1239-1254.
- Burkhardt JK, Echeverri CJ, Nilsson T, Vallee RB. Overexpression of the dynactin (p50) subunit of the dynactin complex disrupts dynein-dependent maintenance of membrane organelle distribution. *J Cell Biol* 1997; **139**:469-484.
- Beckerle MC, Porter KR. Inhibitors of dynein activity block intracellular transport in erythrocytes. *Nature* 1982;



- 295:701-703.
- 35 Ravikumar B, Acevedo-Arozena A, Imarisio S, *et al.* Dynein mutations impair autophagic clearance of aggregate-prone proteins. *Nat Genet* 2005; **37**:771-776.
- 36 Katsumata K, Nishiyama J, Inoue T, Mizushima N, Takeda J, Yuzaki M. Dynein- and activity-dependent retrograde transport of autophagosomes in neuronal axons. *Autophagy* 2010; **6**:378-385.
- 37 Sachdev P, Menon S, Kastner DB, *et al.* G protein beta gamma subunit interaction with the dynein light-chain component Tctex-1 regulates neurite outgrowth. *EMBO J* 2007; **26**:2621-2632.
- 38 Ardley HC, Scott GB, Rose SA, Tan NG, Markham AF, Robinson PA. Inhibition of proteasomal activity causes inclusion formation in neuronal and non-neuronal cells overexpressing Parkin. *Mol Biol Cell* 2003; **14**:4541-4556.
- 39 Shan Y, Yu L, Li Y, *et al.* Nudel and FAK as antagonizing strength modulators of nascent adhesions through paxillin. *PLoS Biol* 2009; **7**:e1000116.
- 40 Steffen W, Karki S, Vaughan KT, *et al.* The involvement of the intermediate chain of cytoplasmic dynein in binding the motor complex to membranous organelles of *Xenopus* oocytes. *Mol Biol Cell* 1997; **8**:2077-2088.
- 41 Wang S, Zheng Y. Identification of a novel dynein binding domain in nudel essential for spindle pole organization in *Xenopus* egg extract. *J Biol Chem* 2011; **286**:587-593.
- 42 Ni Y, Zhao X, Bao G, *et al.* Activation of beta2-adrenergic receptor stimulates gamma-secretase activity and accelerates amyloid plaque formation. *Nat Med* 2006; **12**:1390-1396.
- 43 Johnston JA, Ward CL, Kopito RR. Aggresomes: a cellular response to misfolded proteins. *J Cell Biol* 1998; **143**:1883-1898.
- 44 Wigley WC, Fabunmi RP, Lee MG, *et al.* Dynamic association of proteasomal machinery with the centrosome. *J Cell Biol* 1999; **145**:481-490.
- 45 Badano JL, Teslovich TM, Katsanis N. The centrosome in human genetic disease. *Nat Rev Genet* 2005; **6**:194-205.
- 46 Fabunmi RP, Wigley WC, Thomas PJ, DeMartino GN. Activity and regulation of the centrosome-associated proteasome. *J Biol Chem* 2000; **275**:409-413.
- 47 Zhang J, Liu W, Liu J, *et al.* G-protein beta2 subunit interacts with mitofusin 1 to regulate mitochondrial fusion. *Nat Commun* 2010; **1**:101.
- 48 Taylor JP, Tanaka F, Robitschek J, *et al.* Aggresomes protect cells by enhancing the degradation of toxic polyglutamine-containing protein. *Hum Mol Genet* 2003; **12**:749-757.
- 49 Yang ZY, Guo J, Li N, Qian M, Wang SN, Zhu XL. Mitosin/CENP-F is a conserved kinetochore protein subjected to cytoplasmic dynein-mediated poleward transport. *Cell Res* 2003; **13**:275-283.
- 50 Hoffman DB, Pearson CG, Yen TJ, Howell BJ, Salmon ED. Microtubule-dependent changes in assembly of microtubule motor proteins and mitotic spindle checkpoint proteins at PtK1 kinetochores. *Mol Biol Cell* 2001; **12**:1995-2009.
- 51 Yan X, Zhao X, Qian M, Guo N, Gong X, Zhu X. Characterization and gene structure of a novel retinoblastoma-protein-associated protein similar to the transcription regulator TFII-I. *Biochem J* 2000; **345 (Part 3)**:749-757.
- 52 Schagger H. Tricine-SDS-PAGE. *Nat Protoc* 2006; **1**:16-22.
- 53 Bonifacino JS. Metabolic labeling with amino acids. *Curr Protoc Protein Sci* 2001; **Chapter 3**:Unit 3.7.

(Supplementary information is linked to the online version of the paper on the *Cell Research* website.)